LETTERS

Mouse development with a single E2F activator

Shih-Yin Tsai[1,2,3]*, Rene Opavsky[1,2,3]*, Nidhi Sharma[1,2,3]*, Lizhao Wu[1,2,3]†, Shan Naidu[2,3,4], Eric Nolan[1,2,3], Enrique Feria-Arias[1,2,3], Cynthia Timmers[1,2,3], Jana Opavska[1,2,3], Alain de Bruin[1,2,3], Jean-Leon Chong[1,2,3], Prashant Trikha[1,2,3], Soledad A. Fernandez[5], Paul Stromberg[4], Thomas J. Rosol[4] & Gustavo Leone[1,2,3]

The E2F family is conserved from *Caenorhabditis elegans* to mammals, with some family members having transcription activation functions and others having repressor functions[1,2]. Whereas *C. elegans*[3] and *Drosophila melanogaster*[4,5] have a single E2F activator protein and repressor protein, mammals have at least three activator and five repressor proteins[1,2,6]. Why such genetic complexity evolved in mammals is not known. To begin to evaluate this genetic complexity, we targeted the inactivation of the entire subset of activators, *E2f1*, *E2f2*, *E2f3a* and *E2f3b*, singly or in combination in mice. We demonstrate that *E2f3a* is sufficient to support mouse embryonic and postnatal development. Remarkably, expression of *E2f3b* or *E2f1* from the *E2f3a* locus (*E2f3a*^{3bki} or *E2f3a*^{1ki}, respectively) suppressed all the postnatal phenotypes associated with the inactivation of *E2f3a*. We conclude that there is significant functional redundancy among activators and that the specific requirement for *E2f3a* during postnatal development is dictated by regulatory sequences governing its selective spatiotemporal expression and not by its intrinsic protein functions. These findings provide a molecular basis for the observed specificity among E2F activators during development.

Since the identification of the founding E2F family member, *E2f1* (ref. 7), two distinct genes in nematodes and flies and eight genes in mammals have been identified to encode the signature DNA binding domain that endow these transcription factors with E2F classification[1,2,6]. Among the mammalian E2F activator subset, the *E2f3* gene has emerged as the critical family member involved in the control of cell proliferation and development[8,9]. The *E2f3* locus was originally thought to encode a single DNA binding activity, but was later shown to drive the expression of two related isoforms, *E2f3a* and *E2f3b*, from two distinct promoters[10]. Given the critical link between the *E2f3* locus and the control of cell proliferation, we used homologous recombination to disrupt individually its two isoforms in mice and rigorously evaluate how their functions are integrated with that of other E2F activators. The inactivation of *E2f3a* or *E2f3b* was achieved by targeting exon 1a or 1b sequences, respectively, using Cre/*loxP* technology (Fig. 1a). Mice deleted for either exon 1a or exon 1b were identified by Southern blot and genomic polymerase chain reaction (PCR) analysis (Fig. 1b). Specific ablation of *E2f3a* or *E2f3b* was confirmed by western blot assays using total E2F3-specific antibodies (Fig. 1c).

It was previously shown that inactivation of both *E2f3a* and *E2f3b* (*E2f3*$^{-/-}$) in mice with a mixed strain background yielded offspring that developed rather normally[8,9], but we show here that breeding these mice into a pure strain background (~98% pure) resulted in embryonic lethality (Fig. 1e and Supplementary Fig. 1). Intercrossing *E2f3*$^{+/-}$ mice of different pure backgrounds restored viability of

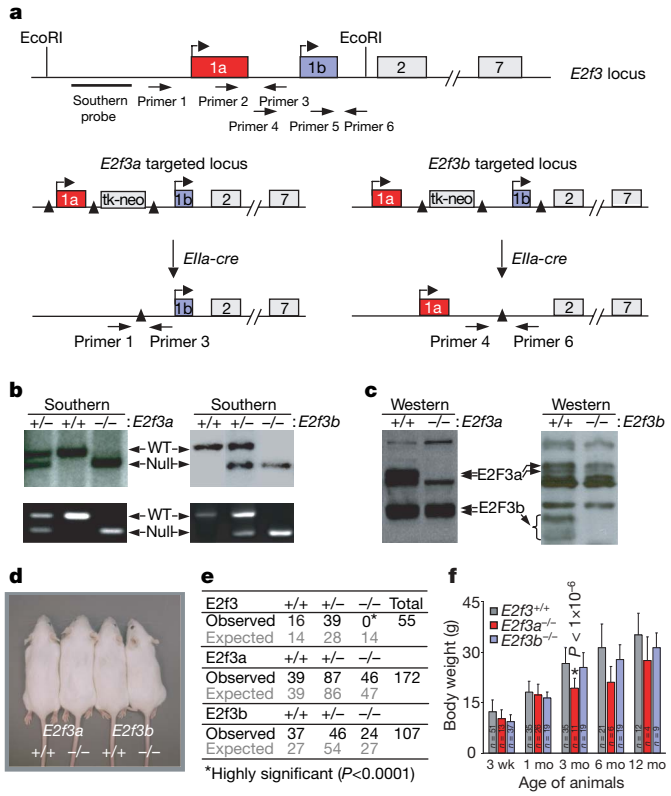

Figure 1 | Generation of *E2f3a* and *E2f3b* knockout mice. **a**, Partial exon/intron structure of the mouse *E2f3* gene. The schematic illustrates the *E2f3* locus with two separate promoters driving the expression of *E2f3a* and *E2f3b*. The two transcription start sites are indicated by bent arrows. The targeting vectors and the final *E2f3a* and *E2f3b* targeted alleles are shown on the left and right, respectively. The solid bar represents a HindIII-BamHI fragment used as the Southern probe. The *loxP* sites are indicated as solid triangles; PCR primers are indicated by arrows. **b**, Southern blot (top panels) and PCR genotyping assays (bottom panels) were performed on MEFs with the indicated genotypes. **c**, Western blot analysis using E2F3-specific antibodies was performed on lysates derived from MEFs with the indicated genotypes. **d**, Micrograph of 1-month-old mice with the indicated genotypes. **e**, Genotypic analysis of offspring derived from *E2f3*$^{+/-}$, *E2f3a*$^{+/-}$ and *E2f3b*$^{+/-}$ intercrosses (fifth generation FVB). A Fisher exact probability test was performed on each genetic group in comparison to the wild-type group; highly significant results are indicated by an asterisk. **f**, Body weights of *E2f3*$^{+/+}$ (grey), *E2f3a*$^{-/-}$ (red) and *E2f3b*$^{-/-}$ (blue) mice at the indicated ages; *n*, number of animals measured for each genotype at each age; error bars represent deviations within each genetic group. A Student's *t*-test was performed on each genetic group in comparison to the wild-type group. Highly significant results are indicated by an asterisk.

[1]Department of Molecular Genetics, College of Biological Sciences, [2]Human Cancer Genetics Program, Comprehensive Cancer Center, [3]Department of Molecular Virology Immunology and Medical Genetics, College of Medicine, [4]Department of Veterinary Biosciences, College of Veterinary Medicine, and [5]Center for Biostatistics, The Ohio State University, Columbus, Ohio 43210, USA. †Present address: Department of Cell Biology and Molecular Medicine and University Hospital Cancer Center, UMDNJ-New Jersey Medical School, Newark, New Jersey 07103, USA.
*These authors contributed equally to this work.

E2f3$^{-/-}$ mice, albeit with some observed strain-specific biases (Supplementary Fig. 1). In contrast, the ablation of individual *E2f3* isoforms (*E2f3a*$^{-/-}$ or *E2f3b*$^{-/-}$) in a pure strain background yielded live pups at the expected mendelian frequency (Fig. 1d–f). These results suggest that *E2f3a* and *E2f3b* have redundant functions during

a

Genotype	*3a*$^{+/+}$	*3a*$^{+/-}$	*3a*$^{-/-}$	*3a*$^{+/+}$	*3a*$^{+/-}$	*3a*$^{-/-}$	*3a*$^{+/+}$	*3a*$^{+/-}$	*3a*$^{-/-}$	Total
	E2f1$^{+/+}$			*E2f1*$^{+/-}$			*E2f1*$^{-/-}$			
Newborn	25	54	37	32	172	114	32	83	39(5)	624
Expected	29	72	43	35	156	99	35	78	49	
21 days	23	54	36	59	164	110	27	74	19*	566
Expected	25	65	39	57	142	91	32	71	45	
Genotype	*3a*$^{+/+}$	*3a*$^{+/-}$	*3a*$^{-/-}$	*3a*$^{+/+}$	*3a*$^{+/-}$	*3a*$^{-/-}$	*3a*$^{+/+}$	*3a*$^{+/-}$	*3a*$^{-/-}$	Total
	E2f2$^{+/+}$			*E2f2*$^{+/-}$			*E2f2*$^{-/-}$			
21 days	0	5	2	9	14	9	4	11	7	61
Expected	2	6	3	6	14	8	3	11	8	
Genotype	*E2f3a*$^{+/+}$			*E2f3a*$^{+/-}$			*E2f3a*$^{-/-}$			Total
	E2f1$^{-/-}$*E2f2*$^{-/-}$			*E2f1*$^{-/-}$*E2f2*$^{-/-}$			*E2f1*$^{-/-}$*E2f2*$^{-/-}$			
E13.5	–			5			9			161
Expected	–			19			17			
E17.5	0			1			4			38
Expected	0			1			4			
E18.5	0			1			2(3)			43
Expected	0			1			5			
Newborn	3			11			0*(4)			275
Expected	3			13			13			

*Highly significant (P<0.05)

b

Genotype	*3b*$^{+/+}$	*3b*$^{+/-}$	*3b*$^{-/-}$	*3b*$^{+/+}$	*3b*$^{+/-}$	*3b*$^{-/-}$	*3b*$^{+/+}$	*3b*$^{+/-}$	*3b*$^{-/-}$	Total
	E2f1$^{+/+}$			*E2f1*$^{+/-}$			*E2f1*$^{-/-}$			
21 days	27	39	18	45	76	34	17	48	24	328
Expected	21	41	21	41	82	41	21	41	21	
Genotype	*3b*$^{+/+}$	*3b*$^{+/-}$	*3b*$^{-/-}$	*3b*$^{+/+}$	*3b*$^{+/-}$	*3b*$^{-/-}$	*3b*$^{+/+}$	*3b*$^{+/-}$	*3b*$^{-/-}$	Total
	E2f2$^{+/+}$			*E2f2*$^{+/-}$			*E2f2*$^{-/-}$			
21 days	11	17	10	20	34	16	11	24	8	156
Expected	8	18	10	18	39	21	10	21	12	
Genotype	*E2f3b*$^{+/+}$			*E2f3b*$^{+/-}$			*E2f3b*$^{-/-}$			Total
	E2f1$^{-/-}$*E2f2*$^{-/-}$			*E2f1*$^{-/-}$*E2f2*$^{-/-}$			*E2f1*$^{-/-}$*E2f2*$^{-/-}$			
E13.5	–			1			2			58
Expected	–			1			3			
Newborn	0			0			2			45
Expected	0			1			2			

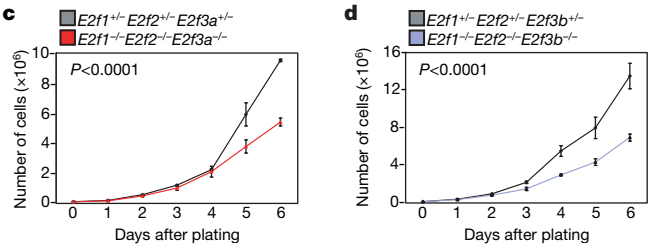

Figure 2 | Genotypic analysis of embryos and offspring deficient for various combinations of activating E2Fs. **a**, Genotypic analysis of offspring deficient for *E2f1*, *E2f2* and *E2f3a* (*3a*); highly significant results are indicated by an asterisk. Numbers in parentheses represent dead embryos/pups. **b**, Genotypic analysis of offspring deficient for *E2f1*, *E2f2* and *E2f3b* (*3b*). **c**, Growth curves of *E2f1*$^{-/-}$*E2f2*$^{-/-}$*E2f3a*$^{-/-}$ (red) and littermate control MEFs (grey). Four independent primary MEF lines of each genotype were plated in duplicate and counted every day for 6 days; a representative experiment is presented in **c**, where the error bars represent deviations between duplicate measurements within the same experiment. **d**, Growth curves of *E2f1*$^{-/-}$*E2f2*$^{-/-}$*E2f3b*$^{-/-}$ (blue) and littermate control MEFs (grey). Two independent primary MEF lines of each genotype were plated in duplicate and counted every day for 6 days; the entire experiment was performed twice and a representative experiment is presented in **d**, where the error bars represent deviations between duplicate measurements within the same experiment. For the cell proliferation studies in **c**, **d**, a generalized linear model (GLM) was used to study the association between cell proliferation and group behaviour, combining the data from all experiments in each genetic study. The *P*-value shown in the graphs corresponds to the main 'group effect' (see Methods).

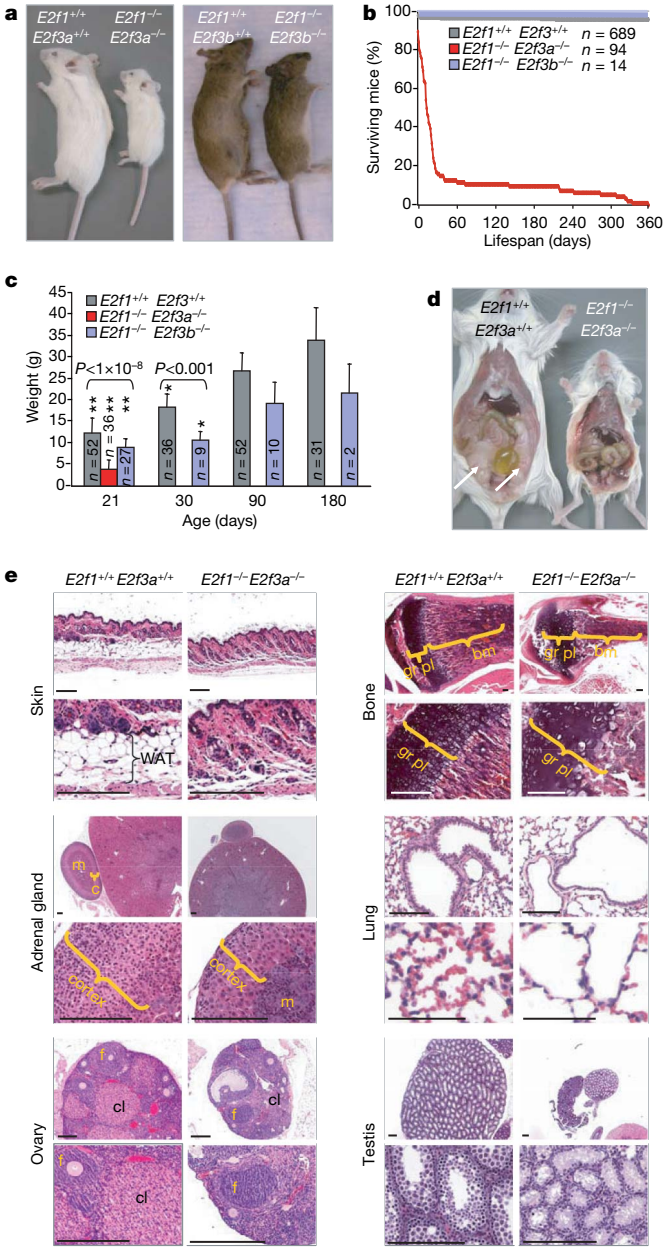

Figure 3 | *E2f1* and *E2f3a* are essential for postnatal development. **a**, Micrograph of *E2f1*$^{+/+}$*E2f3a*$^{+/+}$, *E2f1*$^{-/-}$*E2f3a*$^{-/-}$, *E2f1*$^{+/+}$*E2f3b*$^{+/+}$ and *E2f1*$^{-/-}$*E2f3b*$^{-/-}$ 30-day-old mice. **b**, Survival graph of mice with the indicated genotypes over a period of 1 year. **c**, Body weight of mice with the indicated genotypes and ages; *E2f1*$^{+/+}$*E2f3*$^{+/+}$ represent mice that were pooled from the *E2f1*$^{+/+}$*E2f3a*$^{+/+}$ and *E2f1*$^{+/+}$*E2f3b*$^{+/+}$ genetic groups; *n*, number of animals measured for each genotype; error bars represent deviations within each genetic group. A Student's *t*-test was performed on each genetic group in comparison to the wild-type group. Significant and highly significant results are indicated by a single and double asterisk, respectively. **d**, Micrograph of *E2f1*$^{+/+}$*E2f3a*$^{+/+}$ and *E2f1*$^{-/-}$*E2f3a*$^{-/-}$ 30-day-old mice with an open abdominal cavity; Inguinal WAT in the wild-type mouse is indicated by the white arrows; note the absence of WAT in the mutant mouse. **e**, Haematoxylin and eosin stained tissue sections of 21-day-old (unless indicated) *E2f1*$^{+/+}$*E2f3a*$^{+/+}$ and *E2f1*$^{-/-}$*E2f3a*$^{-/-}$ mice. Top left: skin sections; note the complete absence of WAT beneath the skin of the mutant mouse. Middle left: adrenal gland sections; note the reduction of the adrenal cortex in double knockout mutant mice. Bottom left: ovary sections; note the presence of follicles (f) in both genetic groups but the poor development of corpus lutea (cl) in double knockout mutant female mice (6 months of age). Top right: proximal tibia sections; note the disorganization of nuclei in the growth plate (gr pl) of double knockout mutant mice. Middle right: lung sections; note the reduction of alveolar branching in double knockout mutant mice. Bottom right: testis sections; note the reduction in testis size and lack of spermatocytes. Scale bars, 200 μm. bm, bone marrow; c, cortex; m, medulla.

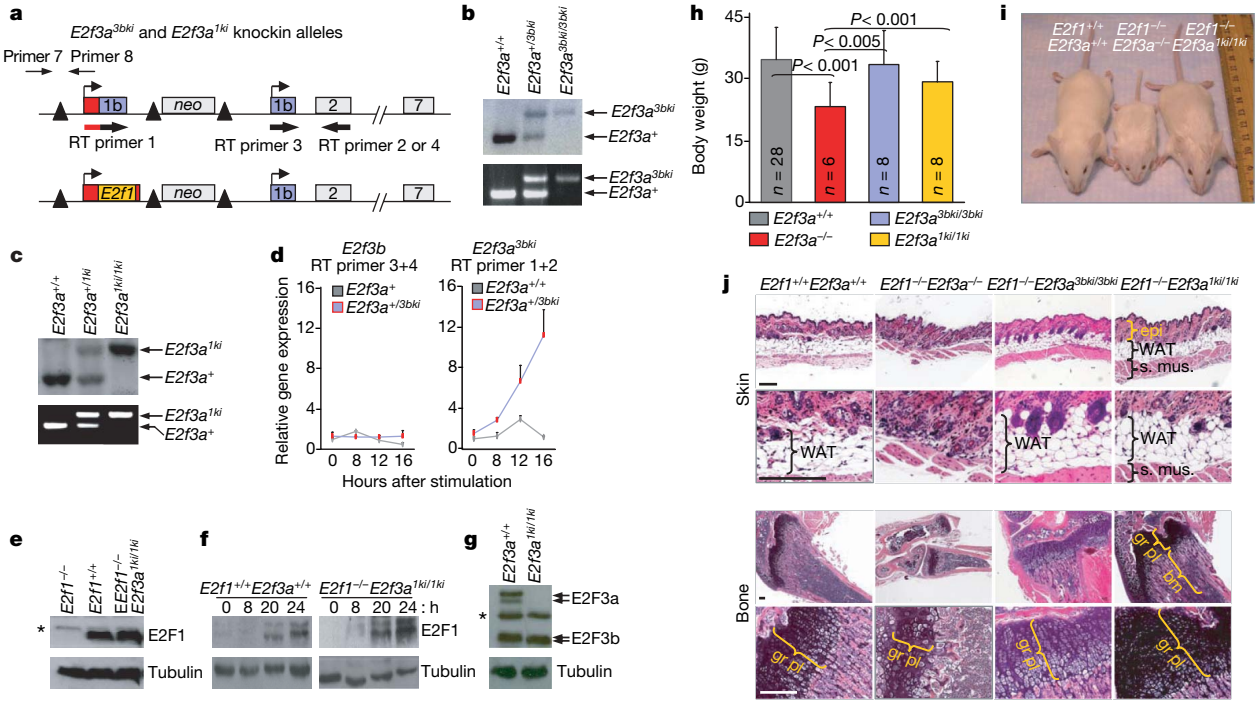

Figure 4 | Expression of *E2f3b* or *E2f1* from the *E2f3a* locus suppresses phenotypes owing to loss of *E2f3a*. **a**, Targeting strategies for replacement of *E2f3a* with *E2f3b* ($E2f3a^{3bki}$; top schematic) or *E2f3a* with *E2f1* ($E2f3a^{1ki}$; bottom schematic). Relevant exons are labelled; *E2f1* indicates the *E2f1* ORF. *loxP* sites are indicated as solid triangles; PCR genotyping primers are indicated by thin arrows; primers for measuring the expression of $E2f3a^{3bki}$ and *E2f3b* alleles by real-time (RT) PCR are indicated by thick arrows. Note that RT primer 1 spans a region that is complementary to exon 1a and exon 1b, as indicated by the red/black coloured arrow. **b**, **c**, Southern blot (top panels) and PCR (bottom panels) genotyping of genomic DNA derived from livers of 1-month-old $E2f3a^{3bki}$ (**b**) and $E2f3a^{1ki}$ (**c**) mice. **d**, Real-time PCR gene expression analysis of the *E2f3b* (left panel) and $E2f3a^{3bki}$ (right panel) alleles in $E2f3a^{+/+}$ (grey square) or $E2f3a^{+/3bki}$ (red/blue square) MEFs. Primers used for each allele are indicated (for primer sequence information see Supplementary Fig. 6). Note that RT primers used to detect $E2f3a^{3bki}$ also detect endogenous *E2f3b* allele as the 3′ portion of RT primer 1 is complementary with exon 1b sequences. Error bars are derived from reactions performed in triplicate. **e**, Western blot analysis of E2F1 protein in proliferating MEFs with the indicated genotypes; α-tubulin was detected as a loading control. Asterisk indicates a nonspecific band. **f**, Western blot analysis of E2F1 proteins in serum stimulated quiescent MEFs having the indicated genotypes; 'h' indicates the time when cells were harvested after stimulation. **g**, Western blot analysis of E2F3a and E2F3b proteins (E2F3 Sc-878) in proliferating MEFs with the indicated genotypes. Asterisk indicates a nonspecific band. **h**, Body weights of 6-month-old $E2f3a^{+/+}$, $E2f3a^{-/-}$, $E2f3a^{3bki/3bki}$ and $E2f3a^{1ki/1ki}$ mice; *n*, number of animals measured for each genotype; error bars represent deviations within each genetic group. Student's *t*-tests were performed between all genetic groups and only significant pair-wise comparisons between groups are indicated by brackets (*P*-values). **i**, Micrograph of 1-month-old $E2f3a^{+/+}$, $E2f1^{-/-}E2f3a^{-/-}$ and $E2f1^{-/-}E2f3a^{1ki/1ki}$ mice. **j**, Haematoxylin and eosin staining of tissue sections of skin and bone from 21-day-old mice with the indicated genotypes. Scale bars, 200 μm. bm, bone marrow; epi, epidermis; gr pl, growth plate; s mus, skeletal muscle.

embryonic development. Because of the functional plasticity that exists among E2F family members[8,11–13], we examined the consequences of inactivating *E2f3a* or *E2f3b* in combination with the other two known E2F activators, *E2f1* and *E2f2*. From the intercrosses described in Fig. 2a, b, we obtained pups doubly deleted for every possible combination of *E2f1*, *E2f2*, *E2f3a* or *E2f1*, *E2f2*, *E2f3b* at or near the expected ratios. Embryos with the two possible triple knockout genotypes ($E2f1^{-/-}E2f2^{-/-}E2f3a^{-/-}$ and $E2f1^{-/-}E2f2^{-/-}E2f3b^{-/-}$) were also obtained at late stages of embryonic development. Given that ablation of all four of these E2F genes in mixed strain background results in early embryonic lethality[8] (G.L., unpublished data), our current findings demonstrate that expression of at least one of the two *E2f3* isoforms is necessary and sufficient to support fetal development in the absence of other E2F activators.

The lack of any obvious proliferative defect in isoform-specific or triple knockout embryos prompted us to examine proliferation more closely in fibroblasts derived from these embryos. To this end, we generated mouse embryo fibroblasts (MEFs) from embryonic day (e)13.5 $E2f3a^{-/-}$, $E2f3b^{-/-}$, $E2f1^{-/-}E2f2^{-/-}E2f3a^{-/-}$ and $E2f1^{-/-}E2f2^{-/-}E2f3b^{-/-}$ embryos and found that all four groups of mutant MEFs had the capacity to proliferate, albeit slightly slower than littermate-derived control MEFs (Fig. 2c, d, Supplementary Fig. 2 and data not shown). Given our previous results showing that a combined deficiency in *E2f1*, *E2f2*, *E2f3a* and *E2f3b* completely abrogates proliferation of MEFs[8], these results suggest a critical and redundant role for the two *E2f3* isoforms in the control of proliferation. It would thus appear that expression of either *E2f3* isoform is sufficient to support cell proliferation as well as embryonic development.

Next we evaluated the role of E2F activators in postnatal development. Mice deficient for each *E2f3* isoform appeared externally normal, were fertile and lived a normal lifespan (Fig. 1d, Supplementary Fig. 3 and data not shown). We did note, however, that older $E2f3a^{-/-}$ mice had less white adipose tissue (WAT) deposition than aged-matched $E2f3b^{-/-}$ or wild-type mice, lending to their thinner appearance (Fig. 1f and data not shown). Given the observed functional redundancy among E2Fs during embryonic development[8,11,14], we reasoned that loss of additional E2F activators might accentuate the rather mild age-dependent phenotype in $E2f3a^{-/-}$ mice. Both $E2f1^{-/-}$ and $E2f2^{-/-}$ mice were previously shown to have a relatively normal lifespan, but with age these mice developed haematopoietic-related complications[15–19]. As shown in Fig. 2a, $E2f2^{-/-}E2f3a^{-/-}$ offspring were born at the expected frequency, had normal birth weights and matured without any obvious additional defects. Newborn $E2f1^{-/-}E2f3a^{-/-}$ pups were also of normal weight and appearance, but by their third week of life the proliferative index in most tissues was significantly reduced (Supplementary Fig. 4b) and mice became severely runted (Fig. 3a–c). The weight of most organs was reduced in double knockout animals, but this decrease was generally proportional to the decrease in their total body weight (Supplementary

Fig. 4a). Gross inspection, however, revealed a total absence of inguinal and subdermal fat (Fig. 3d-e), an observation that was subsequently extended to all WAT deposits in the body. In contrast, brown adipose tissue was relatively unaffected. Analysis of food intake and faecal secretion ruled out a defect in eating behaviour or fat absorption as a cause for the absence of WAT (Supplementary Fig. 4c). Serum triglycerol levels as well as leptin, a major homeostatic regulator of lipid metabolism, were significantly lower in double knockout mice than in control animals (Supplementary Fig. 4d), suggesting a more direct role of E2F3a function in lipid metabolism. Not surprisingly, most $E2f1^{-/-}E2f3a^{-/-}$ pups died within their first month of life, and the few mice that lived longer were severely incapacitated and could be kept alive only by intensive husbandry (Fig. 3b).

Pathological analysis revealed additional organ defects that could account for the growth retardation, general unhealthy disposition and high morbidity of $E2f1^{-/-}E2f3a^{-/-}$ mice. For example, by 21 days of age, the growth plates in long bones of double knockout mice were severely dysplastic with many cells having mega-nuclei that contributed to poor development of trabeculae (Fig. 3e). This was accompanied by a significant decrease in circulating growth hormone and insulin-like growth factor (IGF)-I levels and a relative increase in brain/body weight ratio (Supplementary Fig. 4a, e), providing an interesting parallel to growth hormone deficiency in humans, which causes dwarfism and mainly affects the growth of limbs but not the skull. Moreover, the outer cortex of their adrenal glands lacked a functional zona fasciculata and their lungs were also abnormal, with a decrease in the branching of the epithelium (Fig. 3e). Young mutant males exhibited severe testicular hypoplasia and females had hypoplastic ovaries that lacked a well-developed corpora lutea (Fig. 3e). As a result the few mice that lived past 2 months of age were infertile. We conclude that multi-organ failure resulted in the general deterioration of health and early death of $E2f1^{-/-}E2f3a^{-/-}$ mice. These results illustrate the critical and redundant roles of *E2f1* and *E2f3a* during postnatal development.

In contrast to $E2f1^{-/-}E2f3a^{-/-}$ mice, $E2f1^{-/-}E2f3b^{-/-}$ and $E2f2^{-/-}E2f3b^{-/-}$ progeny developed normally through puberty and adulthood and had a normal lifespan (Fig. 3b and data not shown). Whereas young $E2f1^{-/-}E2f3b^{-/-}$ mice were slightly smaller than wild-type controls (Fig. 3a and 3c), thorough histological examination failed to detect any of the mutant phenotypes observed in $E2f1^{-/-}E2f3a^{-/-}$ animals, including in WAT, bone, adrenal glands, lungs and gonads (data not shown). These observations suggest important differences between *E2f3a* and *E2f3b* during postnatal development. Analysis of $E2f1^{-/-}E2f2^{-/-}E2f3a^{-/-}$ and $E2f1^{-/-}E2f2^{-/-}E2f3b^{-/-}$ triple knockout animals also revealed significant differences between the contribution of *E2f3a* and *E2f3b* towards postnatal development. Whereas both sets of triple knockout embryos could be carried to late stages of gestation, $E2f1^{-/-}E2f2^{-/-}E2f3a^{-/-}$ embryos died perinatally and $E2f1^{-/-}E2f2^{-/-}E2f3b^{-/-}$ pups lived well into adulthood, albeit their body weight was reduced (Fig. 2a, b and data not shown). These findings demonstrate that mouse development can proceed in the presence of a single E2F activator, *E2f3a*.

The different roles of *E2f3a* and *E2f3b* during postnatal development could reflect differences in the function of their gene products or differences in the control of their expression[20–22]. To differentiate between these possibilities we used homologous recombination in mouse embryonic stem cells to replace the coding sequence of exon 1a with the coding sequence of exon 1b ($E2f3a^{3bki}$; Fig. 4a, top panel). We were careful to avoid the inadvertent perturbation of regulatory regions that govern expression from the *E2f3a* locus by leaving the 5′ untranslated region and the 3′ splicing junction of exon 1a intact (Fig. 4b). This strategy resulted in the synthesis of an $E2f3a^{3bki}$ mRNA that was expressed with a similar cell cycle profile as endogenous *E2f3a* and other known E2F targets, without affecting the expression of endogenous *E2f3b* (Fig. 4d). Strikingly, both $E2f3a^{3bki/3bki}$ as well as $E2f1^{-/-}E2f3a^{3bki/3bki}$ mice had normal body weight, WAT deposition, bone structure and growth, adrenal gland morphology and function, as well as normal lung and gonad morphology (Fig. 4h, j, Supplementary Fig. 5 and data not shown). We suggest that the differential requirement for *E2f3a* and *E2f3b* during postnatal development is not based on intrinsic differences between E2F3a and E2F3b protein functions, but rather on differences between how their loci dictate their respective expression.

The above results prompted us to take a similar genetic strategy to determine whether a more distantly related family member, *E2f1*, could also substitute for *E2f3a*. Introduction of the murine *E2f1* coding sequence into exon 1a of the *E2f3a* locus (Fig. 4a bottom panel and Fig. 4c) resulted in the cell-cycle-dependent expression of E2F1 protein (Fig. 4e, f) without affecting expression from the nearby *E2f3b* locus (Fig. 4g). Remarkably, $E2f3a^{1ki/1ki}$ as well as $E2f1^{-/-}E2f3a^{1ki/1ki}$ mice lacked any of the phenotypes caused by a deficiency in *E2f3a* and lived to old age (Fig. 4h–j, Supplementary Fig. 5 and data not shown). Together, these findings suggest that the specific role of *E2f3a* in postnatal development is largely predicated by regulatory sequences governing its spatiotemporal expression pattern. However, we can not rule out specific functions for individual E2Fs in tissues that are not critical for development and that were not analysed here. These observations provide a molecular basis for the observed specificity among E2F family members during development.

Many reasons have been provided to explain why mammals have an expanded E2F family when nematodes and flies have a single E2F activator and a single repressor. Extensive genetic and biochemical analysis using cell culture systems has demonstrated that different E2F activators interact with specific cofactors and elicit different biological responses[23–25]. These studies inspired the view that the complexity of the mammalian E2F family affords a more complex and presumably better equipped organism to develop, but *in vivo* evidence in support of this hypothesis has been lacking. The *in vivo* analyses presented here provide new perspectives to this old problem. Our current findings suggest that biological processes regulated by E2F during development in nematodes, flies and mammals are more alike than previously anticipated because, like in nematodes and flies, a single E2F activator (*E2f3a*) is sufficient to support development in the mouse. The surprising observation that E2F3a protein function during postnatal development can be substituted equally well by either the structurally related E2F3b or the more distantly related E2F1 proteins highlights the critical nature of *E2f3a* regulatory sequences for postnatal development. It would appear that beyond broadening gene expression patterns, the mammalian genome has gained little developmental currency by the acquisition of additional E2F family members. It remains possible that the evolution of multiple E2Fs in mammals might represent an adaptation that could serve, beyond simply broadening expression patterns, to meet the challenges faced by ageing animals reared in their natural habitat.

METHODS SUMMARY

Construction of *E2f3a*, *E2f3b*, $E2f3a^{3bki}$ and $E2f3a^{1ki}$ targeting vectors. The triple *loxP* vector system and standard cloning techniques were used to construct all targeting vectors[8] (see Supplementary Information for details).

Generation of $E2f3a^{-/-}$, $E2f3b^{-/-}$, $E2f3a^{3bki/3bki}$ and $E2f3a^{1ki/1ki}$ mice. TC1 129Sv/Ev ES cells were electroporated with 50 μg of NotI-linearized targeting vectors. Homologous recombination was selected with G418 and ganciclovir and verified by Southern blotting using 5′ and 3′ external probes. Appropriate ES clones were injected into e3.5 C57BL/6 blastocysts that were subsequently implanted into foster mothers. We bred the resulting chimaeras with NIH black Swiss females and selected agouti offspring for genotyping. Offspring with germline transmission of the *E2f3a* or *E2f3b* targeted alleles were bred with *EIIa-cre* mice to excise exon 1a or exon 1b, respectively, as well as the neomycin cassette.

Genotyping of knockout and knockin mice. Genotyping of offspring was performed by PCR and Southern blot analysis. Southern blots analysis was performed using genomic DNA digested with EcoRI and a ^{32}P-labelled HindIII-BamHI fragment as the hybridization probe. The wild type, *E2f3a* and *E2f3b* knockout, as well as the $E2f3a^{3bki}$ and $E2f3a^{1ki}$ alleles, yielded fragments of approximately 6 kb, 5.2 kb, 4.4 kb, 7 kb and 9 kb, respectively. Homozygous mice

were obtained by interbreeding heterozygous mice of each genotype. Multiplex PCR for genotyping used three primers for *E2f3a* (primer 1, primer 2, primer 3) and *E2f3b* (primer 4, primer 5, primer 6), and the same two primers for $E2f3a^{3bki}$ and $E2f3a^{1ki}$ (primer 7; primer 8). Primer sequences are listed in Supplementary Fig. 6.

Full Methods and any associated references are available in the online version of the paper at www.nature.com/nature.

Received 6 November 2007; accepted 7 May 2008.
Published online 25 June 2008.

1. Trimarchi, J. M. & Lees, J. A. Sibling rivalry in the E2F family. *Nature Rev. Mol. Cell Biol.* **3,** 11–20 (2002).
2. Attwooll, C., Lazzerini Denchi, E. & Helin, K. The E2F family: specific functions and overlapping interests. *EMBO J.* **23,** 4709–4716 (2004).
3. Ceol, C. J. & Horvitz, H. R. dpl-1 DP and efl-1 E2F act with lin-35 Rb to antagonize Ras signaling in *C. elegans* vulval development. *Mol. Cell* **7,** 461–473 (2001).
4. Dynlacht, B. D., Brook, A., Dembski, M., Yenush, L. & Dyson, N. DNA-binding and trans-activation properties of *Drosophila* E2F and DP proteins. *Proc. Natl Acad. Sci. USA* **91,** 6359–6363 (1994).
5. Sawado, T. *et al.* dE2F2, a novel E2F-family transcription factor in *Drosophila melanogaster*. *Biochem. Biophys. Res. Commun.* **251,** 409–415 (1998).
6. DeGregori, J. & Johnson, D. G. Distinct and overlapping roles for E2F family members in transcription, proliferation and apoptosis. *Curr. Mol. Med.* **6,** 739–748 (2006).
7. Helin, K. *et al.* A cDNA encoding a pRB-binding protein with properties of the transcription factor E2F. *Cell* **70,** 337–350 (1992).
8. Wu, L. *et al.* The E2F1–3 transcription factors are essential for cellular proliferation. *Nature* **414,** 457–462 (2001).
9. Humbert, P. O. *et al.* E2f3 is critical for normal cellular proliferation. *Genes Dev.* **14,** 690–703 (2000).
10. Leone, G. *et al.* Identification of a novel E2F3 product suggests a mechanism for determining specificity of repression by Rb proteins. *Mol. Cell. Biol.* **20,** 3626–3632 (2000).
11. Li, J. *et al.* Synergistic function of E2F7 and E2F8 is essential for cell survival and embryonic development. *Dev. Cell* **14,** 62–75 (2008).
12. Giangrande, P. H. *et al.* A role for E2F6 in distinguishing G1/S- and G2/M-specific transcription. *Genes Dev.* **18,** 2941–2951 (2004).
13. Cloud, J. E. *et al.* Mutant mouse models reveal the relative roles of E2F1 and E2F3 *in vivo*. *Mol. Cell. Biol.* **22,** 2663–2672 (2002).
14. Gaubatz, S. *et al.* E2F4 and E2F5 play an essential role in pocket protein-mediated G1 control. *Mol. Cell* **6,** 729–735 (2000).
15. Yamasaki, L. *et al.* Tumor induction and tissue atrophy in mice lacking E2F–1. *Cell* **85,** 537–548 (1996).
16. Murga, M. *et al.* Mutation of E2F2 in mice causes enhanced T lymphocyte proliferation, leading to the development of autoimmunity. *Immunity* **15,** 959–970 (2001).
17. Field, S. J. *et al.* E2F-1 functions in mice to promote apoptosis and suppress proliferation. *Cell* **85,** 549–561 (1996).
18. Zhu, J. W. *et al.* E2F1 and E2F2 determine thresholds for antigen-induced T-cell proliferation and suppress tumorigenesis. *Mol. Cell. Biol.* **21,** 8547–8564 (2001).
19. Li, F. X., Zhu, J. W., Hogan, C. J. & DeGregori, J. Defective gene expression, S phase progression, and maturation during hematopoiesis in E2F1/E2F2 mutant mice. *Mol. Cell. Biol.* **23,** 3607–3622 (2003).
20. Opavsky, R. *et al.* Specific tumor suppressor function for E2F2 in Myc-induced T cell lymphomagenesis. *Proc. Natl Acad. Sci. USA* **104,** 15400–15405 (2007).
21. Dirlam, A., Spike, B. T. & Macleod, K. F. Deregulated E2f-2 underlies cell cycle and maturation defects in retinoblastoma null erythroblasts. *Mol. Cell. Biol.* **27,** 8713–8728 (2007).
22. Parisi, T. *et al.* Selective requirements for E2f3 in the development and tumorigenicity of Rb-deficient chimeric tissues. *Mol. Cell. Biol.* **27,** 2283–2293 (2007).
23. Blais, A. & Dynlacht, B. D. E2F-associated chromatin modifiers and cell cycle control. *Curr. Opin. Cell Biol.* **19,** 658–662 (2007).
24. Giangrande, P. H., Hallstrom, T. C., Tunyaplin, C., Calame, K. & Nevins, J. R. Identification of E-box factor TFE3 as a functional partner for the E2F3 transcription factor. *Mol. Cell. Biol.* **23,** 3707–3720 (2003).
25. Schlisio, S., Halperin, T., Vidal, M. & Nevins, J. R. Interaction of YY1 with E2Fs, mediated by RYBP, provides a mechanism for specificity of E2F function. *EMBO J.* **21,** 5775–5786 (2002).

Supplementary Information is linked to the online version of the paper at www.nature.com/nature.

Acknowledgements We thank J. Moffitt and L. Rawahneh for histology expertise. We also thank J. Nevins, C. Bock and A. Otoshi for support in the generation of the *E2f3a*, *E2f3b*, $E2f3a^{3bki}$ and $E2f3a^{1ki}$ mice, and the Mouse Metabolic Phenotyping center at the University of Cincinnati for advice on the analysis of $E2f1^{-/-}E2f3a^{-/-}$ mice. We are grateful to D. Guttridge, M. Ostrowski and M. Simcox for critically reading the manuscript and helpful suggestions. This work was funded by NIH grants to G.L. (R01CA85619, R01HD042619, R01CA121275, R01HD047470, P01CA097189), to L.W. (K01CA102328), DoD awards to A.d.B. (BC0300893) and J.-L.C. (BC061730), and a T32 fellowship (CA106196) to R.O. G.L. is the recipient of the Pew Charitable Trusts Scholar Award and the Leukemia and Lymphoma Society Scholar Award.

Author Information Reprints and permissions information is available at www.nature.com/reprints. Correspondence and requests for materials should be addressed to G.L. (Gustavo.Leone@osumc.edu).

METHODS

Construction of *E2f3a*, *E2f3b*, *E2f3a^{3bki}* and *E2f3a^{1ki}* targeting vectors. The *E2f3a* knockout vector contained a neo cassette flanked by *loxP* sites, which was inserted into the HaeII restriction site 108 bp upstream of the *E2f3a* starting codon. An additional *loxP* site was inserted into the HindIII site ~300 bp downstream of exon 1a. The two arms of homology used for recombination included a total 3.1-kb HindIII-EcoRI fragment upstream of the neo cassette and a 900-bp fragment downstream of the 3′ *loxP* site. For the *E2f3b* knockout targeting vector, the same *loxP*–flanked neo cassette was inserted ~800 bp upstream of exon 1b and an additional *loxP* site was inserted ~1.8 kb downstream of exon 1b. The two arms of homology used for recombination included a 1-kb HindIII-HindIII fragment upstream of the neo cassette and a 9-kb EcoRI-XhoI fragment downstream of the 3′ *loxP* site. The *E2f3a^{3bki}* and *E2f3a^{1ki}* knockin constructs were identical to the *E2f3a* knockout construct described above with the following exceptions. For the *E2f3a^{3bki}* construct, the exon 1b open reading frame (ORF) was replaced with the exon 1a ORF. For the *E2f3a^{1ki}* construct, the *E2f1* ORF carrying its own termination codon was inserted downstream of the first ATG in exon 1a. All the final targeting vectors were confirmed by direct DNA sequencing.

Fat absorption assay. Fat absorption assays were performed on 1-month-old mice at the mouse metabolic phenotyping centre at the University of Cincinnati as described previously[26].

Blood serum analysis. Mice at 21 days of age were killed and serum was collected from blood by centrifugation at 6,000*g*. The serum was then stored at −80 °C until further analysis. Triglycerides, cholesterol and leptin were analysed by the Mouse Metabolic Phenotyping Center at the University of Cincinnati. Analysis of serum growth hormone and IGF-I was performed at the Vanderbilt hormone assays and analytical core services.

Generation of MEFs and cell culture conditions. Primary MEFs were isolated from e13.5 embryos using standard methods[8]. MEFs were cultured in DMEM with 15% fetal bovine serum (FBS). Proliferation assays were performed by plating MEFs at 1.45×10^5 cells per 60-mm dish. Duplicate plates were counted daily using a Beckton Dickson Coulter Counter and were re-plated 72 h after at the same initial density. Four independent *E2f1$^{-/-}$ E2f2$^{-/-}$ E2f3a$^{-/-}$* MEF lines and two independent *E2f1$^{-/-}$ E2f2$^{-/-}$ E2f3b$^{-/-}$* MEF lines with their control littermate were used in the proliferation assays. Statistical analysis was performed by pooling all experiments.

Protein and RNA analysis. Cells were scraped from culture dishes in chilled PBS, centrifuged, and washed once with ice-cold PBS. Total protein extracts were prepared by incubating cells in RIPA extraction buffer for 30 min on ice. Total protein was then separated by SDS–PAGE and transferred to PVDF membranes. Blots were probed with antibodies specific for E2F3 (Santa Cruz Sc-878) or E2F1 (Santa Cruz Sc-193); anti-α-tubulin (Sigma T6199) was used to determine protein loading. Total RNA was extracted from MEFs using Qiagen RNeasy mini kit. Reverse transcription of 2 μg of total RNA was performed by combining 1 μl of Superscript III reverse transcriptase (Invitrogen), 4 μl of 5× buffer, 0.5 μl of 100 mM oligo dT primer, 0.5 μl of 25 mM dNTPs, 1.0 μl of 0.1 M dithiothreitol, 1.0 μl of RNase Inhibitor (Roche) and water up to a volume of 20 μl. Reactions were incubated at 50 °C for 60 min and then diluted fivefold with 80 μl of water. Real-time RT–PCR was performed using the BioRad iCycler PCR machine. Each PCR reaction contained 0.5 μl of cDNA template and primers at a concentration of 100 nM in a final volume of 25 μl of SYBR green reaction mix (BioRad). Each PCR reaction yielded only the expected amplicon as shown by the melting-temperature profiles of the final products and by gel electrophoresis. Standard curves were generated using cDNA to determine the linear range and PCR efficiency of each primer pair. Reactions were performed in triplicate and relative amounts of cDNA were normalized to GAPDH. Primer sequences are listed in Supplementary Fig. 6.

Histopathology and immunohistochemistry. Tissue samples were collected and fixed in 10% neutral formalin. Five-micrometre-thick sections were cut and then stained for with haematoxylin and eosin by standard protocols. Immunohistochemistry using Ki-67-specific antibodies (BD Pharmingen 550609) was performed on paraffin-embedded sections.

Statistical analysis. For the proliferation assays in MEFs, a generalized linear model (GLM) was used to study the association between the outcome variable and group. Time was used as a categorical variable, and the interaction 'time' by 'group' was also included in the model. A fixed effect 'experiment' was included to take into account the differences (or variability) among experiments.

26. Jandacek, R. J., Heubi, J. E. & Tso, P. A novel, noninvasive method for the measurement of intestinal fat absorption. *Gastroenterology* **127,** 139–144 (2004).